Optimization of InP based Photodetectors Fabricated with Generic Photonic Integration Technology

M. Verhage,[1,2] S.C.M. Grijseels,[2] E. den Haan,[2] R. Santos,[2]
K. Voutyras,[2] and L.M. Augustin[2]

[1] Photonics and Semiconductor Physics Group, COBRA Research Institute, Eindhoven University of Technology, 5600 MB Eindhoven, The Netherlands
[2] SMART Photonics, Horsten 1, 5612 AX Eindhoven, The Netherlands

Integrated InP photodetectors are an important building block for photonic integrated circuits. In the SMART Photonics generic integration platform photodetectors are fabricated using a three step epitaxial process. This process allows butt-joint integration of active (photodetectors, gain sections) and passive (waveguides, splitters, couplers, etc.) elements without compromising their performance. Characterization of multi-quantum well InP photodetectors is carried out with electro-optical measurements and theoretical modeling. A design of experiment aims to study the effects of the photodetector's design parameters on the dark current, responsivity, and specific detectivity. These parameters are: width, length, etch-depth, butt-joint direction (orthogonal in-plane direction [011] or [01-1]), and partial or fully extended active multi-quantum well layers across the photodetector's width.

Introduction

An important application of III-V compound semiconductor materials is the development of optoelectronic devices such as photonic emitters and photodiodes (PDs). The design is based on multi quantum well (MQW) semiconductor optical amplifiers (SOAs), operating in the infrared optical telecommunication wavelength regime [1]. Exemplifying that the similarity in design and fabrication allows for easy integration of a wide range of other building block elements. The MQW PDs have, compared to bulk PDs, multiple special merits such as large spectral range and large linearity [2]. The strong exciton absorption at the absorption band edge of the quantum wells results in an increased responsivity [3]. These properties make MQW heterojunction PDs an attractive technology for photonic integrated circuits, of which the development of Indium Phosphide (InP) MQW PDs are especially promising [4, 5].
Dark current, as known, is a primary contributor to noise (noise equivalent power) in photodetectors and influence the responsivity and specific detectivity greatly [6]. For the purpose of high performance PDs, operating at the telecommunication wavelength of 1.55 μm, a small dark current and high responsivity are required. Therefore, a good understanding of dark current mechanisms will pave the way to optimize the design of these PDs. Here, we present a design of experiment (DoE) approach for PDs with different designs. Physical models are applied to describe two different dark current observations and to understand the nature of it. Optimization of the different PD designs in relation to low dark current, high responsivity, and high detectivity, is performed using the DoE.

Experimental setup and photodetector design

The structure under consideration consists of an InP p-*i*-n heterojunction vertical layer

stack. The intrinsic layer is formed of active InGaAsP MQWs, with a net photoluminescence peak of 1.55 µm, which is sandwiched between two confinement layers of Q1.25 InGaAsP material. The photodetector is integrated in an active-passive integration platform and connected to a Q1.25 passive waveguide. The interface between the active and passive layers is referred to as a *butt-joint*. The structure is grown on an n-doped InP substrate. The p-InP and n-InP cladding layers have an equivalent acceptor and donor concentration of 5×10^{17} cm^{-3} at each side of the intrinsic region, gradually increasing toward the p and n contacts. The structure is metallized on top and bottom to bias the PD with an external electric probe.

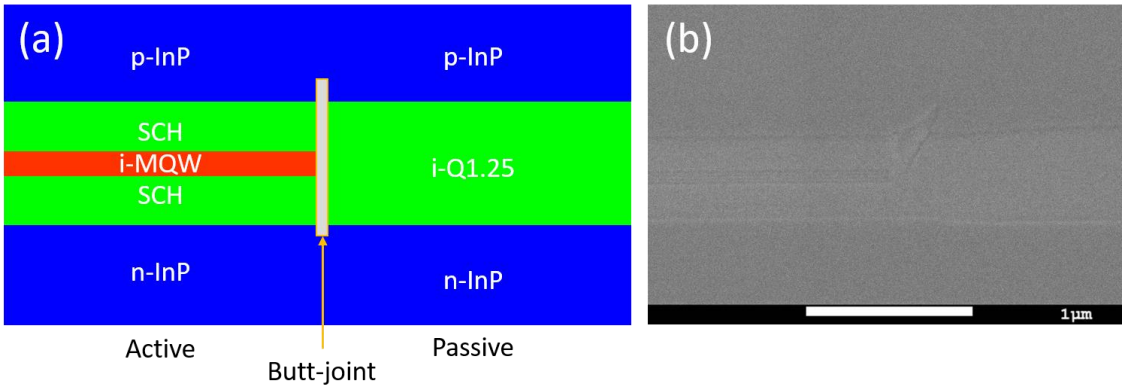

Figure 1(a) Schematic of the device. Indicated in the figure are the Separate Confinement Heterojunction (SCH) layers and the active region. At the interface of the active-passive regions, a butt-joint is formed. (b) A corresponding cross-section SEM image of a butt-joint.

A design of experiment (DoE) is conducted to obtain the PD response to the different factors, i.e., the *variables*, within certain factor levels, i.e., the variable's *range.* The DoE identifies the key factors and optimizes the design with the aim to achieve a certain desired response. The variations of the spatial dimensions of the InP MQW PD layer stack are the factors, which are summarized in Table 1 and drawn in cross-section view in Fig. 2. The design factors and levels are chosen as follows. The PDs differ in length (20 µm, 43 µm, 73 µm, and 100 µm) and width (2 µm, 6 µm, and 10 µm). The rectangular PD arrangement on the die introduces two orthogonal directions referred to as the factor "direction". The factor direction is orthogonally coded in the DoE as 0 and 1, respectively. The factor "etch-depth" is either deep or shallow (1 and 0, respectively), as illustrated in Fig. 2. Finally, the MQW active absorption layers can either extend beyond the width of the PD ("etch-active 1"), or are fully embedded in the Q1.25 material ("etch-active 0"), in which case a butt-joint lies within the PD device.

Etch-depth	0	0	1	1
Etch-active	1	0	1	0

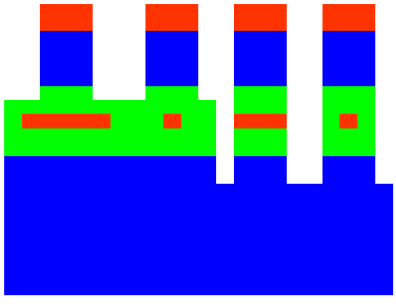

Figure 2 Schematic cross sections of the device DoE. Indicated in the figure are the different layers (also see Fig. 1), and design factors. The top layer (red) is the InGaAs contact layer.

Table 1 Factors and levels in the design of experiment

Factor	Factor Levels
Width (µm)	2, 6, 10
Length (µm)	20, 43, 73, 100
Direction ([011] and [01-1])	0, 1
Etch-depth (shallow and deep)	0, 1
Etch-active (MQWs embedded and extended)	0, 1

Electrical characterization

IV measurements were conducted by a four-point probe setup. This configuration gives high accuracy of current values because of the removed peripheral resistance. A voltage sweep was conducted from 0.5 V to −5.5 V bias, in 150 steps, to measure the current. Two different IV characteristics are consistently observed for all PDs, as illustrated in Fig. 3 for four PDs. Two PDs with etch-active 0, labeled A and B, are of length 20 µm, width 6 µm, etch-depth 1, and have orthogonal orientation. The PDs C and D with etch-active 1, have length 20 µm, width 2 µm, and etch-depth 1 with similar orientation. The dark current measured around 1 V reverse bias is for PD A ~0.4 µA, for PD B ~9 µA, and for the PDs C and D ~0.9 nA. Statistical analysis of the dark current measurements of 80 PDs in the DoE reveals that the design factors etch-active, width, and the two-way interaction term direction × etch-active are the most important factors. The splitting of the IV characteristics is caused by either etching into the active region or etching beyond this region into the passive part of the PD, which make the butt-joints the primary suspect for the enhanced dark current generation of PDs A and B.

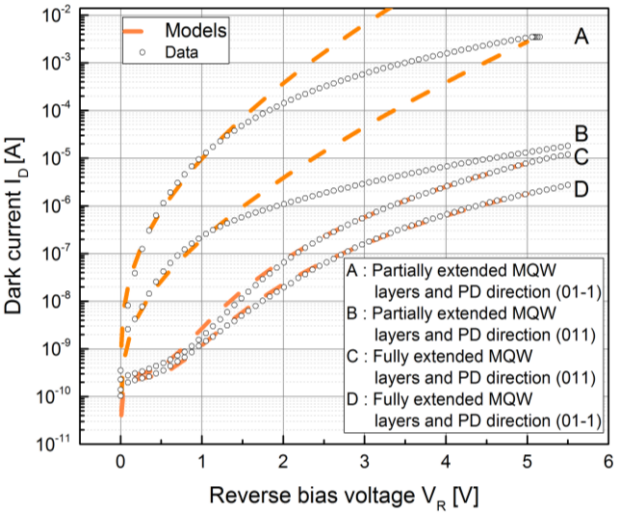

Figure 3 Open points: Measured IV characteristics for four photodetectors showing different dark current behavior. All detectors share the same design parameters, expect for etch-active and direction. Orange lines: modeled dark current.

To explain the observed behavior, the IV characteristics are fitted with two models over four to six orders of magnitude. The first model is based on well-known mechanisms of dark current generation, i.e., the current that emerges from diffusion of minority carriers across the junction, the generation and recombination current of carriers in the depletion region, the band-to-band tunneling, and the trap-assisted tunneling. The second model is based on the Emission-Capture model [7]. Fitting of both models gives insight into the effective lifetime of the carriers, and provide a first order, quantitative approach to calculate the effective trap concentration. It shows that the lifetime of the carriers is much larger (order ~10^2) in the case for the PDs with etch-active 1. Since the lifetime is inversely proportional to the trap concentration, the trap concentration for etch-active 1 is assumed to be much smaller than for etch-active 0. Butt-joints are known to introduce additional traps, originating from crystallographic defects, attributing to the dark current via recombination-generation and trap-assisted tunneling mechanism. The dark current is strongly influenced by the width of the PD, i.e., larger butt-joints, further supporting the contribution of the butt-joints to the dark current. Moreover, the PDs with a fully extended active region, exhibit a gradual increase in dark current for reverse bias voltages below 0.5 V, in accordance with carrier induced band-to-band and/or trap-assisted tunneling mechanisms of dark current generation [8, 9]. On the contrary, for PDs with the factor etch-active 0, a steep increase in dark current at small bias voltages is observed, implying that the generation-recombination mechanism is the dominant dark current generator [10]. The direction of the PD, i.e., the crystal orientation of the butt-joint, has a second order interaction with the factor etch-active. For now, a qualitative explanation of this mechanism is unknown, however it seems that the crystal

orientation (PD direction) increases the number of defects present at the butt-joint. This result underpins the importance of combining the factors etch-active with the direction.

Optical characterization

A similar statistical approach is taken for the investigation of the responsivity. A subset, which is called a fractional factorial design, was chosen to significantly reduce the number of measurements from 80 to 12. DoE of the responsivity shows high dependency on the PD's length, with an optimal design of 100 µm. Fig. 4 shows the responsivity of PDs A and D, taking into account an approximated fiber-to-chip coupling loss of 3 dB. At a wavelength of 1.55 µm both diodes have a responsivity close to 1 A/W.

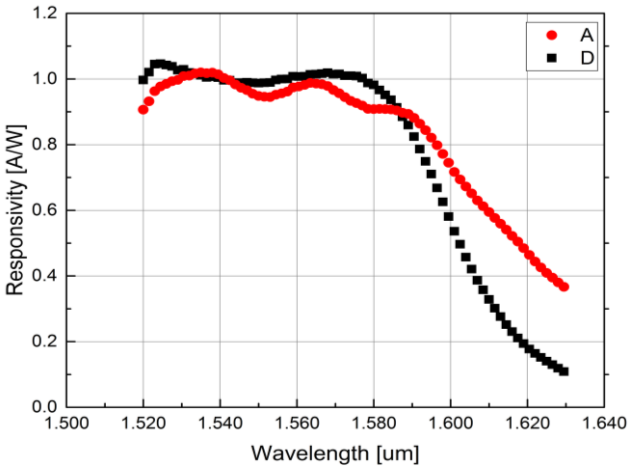

Figure 4 Responsivity of photodetectors A and D at a reverse bias of 3 V. The wavelength is swept from 1520 to 1630 nm.

Conclusion

The DoE performed in this paper shows that minimization of the dark current in the PD can be achieved without affecting its optical performance. This is illustrated by the specific detectivity, which is an important figure of merit to rate the detector performance [11]. It has a linear dependence on the responsivity and is inversely proportional to the square root of the generated noise of the PD. With an optimized design, the specific detectivity was found to be around 8×10^{11} $mHz^{½}W^{-1}$ for PD D at zero bias. These results present the potential in optimizing InP MQW PD's design.

References

[1] M. Verdun, G. Beaudoin, B. Portier, N. Bardou, C. Dupuis, I. Sagnes, R. Haïdar, F. Pardo, and J.-L. Pelouard, "Dark current investigation in thin p-i-n ingaas photodiodes for nano-resonators," J. Appl. Phys., vol. 120, no. 8, 084501, 2016.

[2] K. F. Brennan, J. Haralson, J. W. Parks, and A. Salem, "Review of reliability issues of metal-semiconductor- metal and avalanche photodiode photonic detectors," Microelectron. Reliab., vol. 39, no. 12, 1873 – 1883, 1999.

[3] G. Zhou and P. Runge, "Modeling of multiple-quantum-well p-i-n photodiodes," IEEE J. Quant. Electron., vol. 50, no. 4, pp. 220 – 227, 2014.

[4] M. Smit, *et al.,* "An introduction to InP-based generic integration technology", Semicond. Sci. Tech., vol. 29, no. 8, 083001, 2014.

[5] L.M. Augustin, *et al.*, "InP-Based Generic Foundry Platform for Photonic Integrated Circuits", IEEE J. Sel. Top. Quant., vol. 24, no. 1, 1 – 10, 2018.

[6] B. F. Levine, "Quantum-well infrared photodetector," J. Appl. Phys., vol. 74, no. 8, R1–R81, 1999.

[7] H. Schneider, and H.C. Liu, "Quantum well infrared photodetectors: physics and applications", Berlin, Springer, ch. 4, 51 – 55, 2007.

[8] K. Ohnaka, M. Kubo, and J. Shibata, "A low dark current ingaas/inp p-i-n photodiode with covered mesa structure," IEEE Trans. Electron. Dev., vol. 34, no. 2, 199 – 204, 1987.

[9] B. Chen, J. Yuan, and A. L. Holmes, "Dark current modeling of inp based swir and mwir ingaas/gaassb type-ii ⍑mqw photodiodes," Opt. Quant. Electron., vol. 45, no. 3, 271 – 277, 2013.

[10] Ando, A. B. Fowler, and F. Stern, "Electronic properties of two- [20] dimensional systems," Rev. Mod. Phys., vol. 54, no. 2, 1982.